

# **Vibration Analysis of Two-Directional Functionally Graded Sandwich Beams Using a Shear Deformable Finite Element Formulation**

Vu Nam Pham<sup>1,2</sup>, Dinh Kien Nguyen<sup>2,3,\*</sup>, Buntara Sthenly Gan<sup>4</sup>

<sup>1</sup>ThuyLoi University, 175 Tay Son, Dong Da, Hanoi, Vietnam

<sup>2</sup>Graduate University of Science and Technology, VAST, 18 Hoang Quoc Viet, Hanoi, Vietnam

<sup>3</sup>Institute of Mechanics, VAST, 18 Hoang Quoc Viet, Hanoi, Vietnam

<sup>4</sup>Department of Architecture, College of Engineering, Nihon University, Koriyama, Japan

Received 17 March 2019; received in revised form 10 April 2019; accepted 10 May 2019

## **Abstract**

Free and forced vibration analysis of two-directional functionally graded sandwich (2D-FGSW) beams using a shear deformable finite element formulation is presented. The beams considered in this paper consists of three layers, a homogeneous ceramic core, and two functionally graded skin layers. Material properties of the skin layers are supposed to vary in both the thickness and length directions by power gradation laws. Based on a refined shear deformation beam theory, in which the transverse displacement is split into bending and shear parts, a novel finite element formulation is derived and employed in the analysis. Natural frequencies and dynamic response to a harmonic load of the beams with various boundary conditions are computed, and the influence of the material distribution and the layer thickness ratio on the vibration characteristics of the beams is highlighted. Numerical results reveal that the variation of the material properties in the longitudinal direction has a significant influence on the vibration behavior of the beams, and FGSW beams can be designed to achieve desired vibration characteristics by appropriate selection of material grading indexes.

**Keywords:** 2D-FGSW beam, refined shear deformation theory, vibration analysis, finite element formulation

## **1. Introduction**

Sandwich structures with high strength-to-weight ratio are widely used to fabricate structural elements in aerospace engineering. In order to improve the mechanical performance of these structures under complex loadings, Functionally Graded Materials (FGMs), a new type of composite materials initiated by Japanese researchers in 1984 [1], have been incorporated in the sandwich construction in recent years. Understanding the mechanical behavior of Functionally Graded Sandwich (FGSW) structures in general, and vibration of FGSW beams, in particular, is crucial for using this new composite material effectively. Investigations on the vibration of FGSW beams, the topic discussed in this paper, are briefly discussed below.

Pradhan and Murmu [2] used the modified differential quadrature method to compute natural frequencies of FGSW beams resting on an elastic foundation. The dependence of material properties upon temperature was considered in

The work. Based on the element free Galerkin method, Amirani et al. [3] studied free vibration of an FGSW beam with an FGM core. The authors employed two micromechanics models, Voigt and Mori-Tanaka models, to evaluate the effective material properties of the beams, and they showed that the natural frequencies based on Mori-Tanaka scheme are slightly lower than that using Voigt model. Adopting a hierarchical displacement field, Mashat et al. [4] derived a finite element formulation

---

\* Corresponding author. E-mail address: ndkien@imech.vast.vn

Tel.: +84-24-37628006; Fax: +84-24-37622039

for evaluating natural frequencies of laminated and sandwich beams with material properties varying by a power gradation law. Free vibration and buckling of FGSW beams were considered by Bennai et al. [5] by using a new refined hyperbolic shear deformation beam theory. In [6, 7], Vo et al. presented a refined shear deformation theory and then improved it to form the quasi-3D theory by taking thickness stretching effect into account for studying free vibration and buckling of FGSW beams. Recently, Su et al. [8] employed the modified Fourier series to compute fundamental frequencies of FGSW beams resting on an elastic foundation.

In many practical circumstances, the unidirectional FGM in the above-cited papers may not be so appropriate to resist multi-directional variations of mechanical and thermal loadings, and development of FGM with material properties varying in two or three spatial directions is necessary. Several investigations on vibration analysis of FGM beams with material gradation in both the thickness and length directions have been reported in recent years [9-12]. Investigation on the mechanical behavior of 2D-FGSW beams, however, is still very limited. To the authors' best knowledge, there is only a study by Karamanli in [13], where static bending of FGSW beams with material properties varying in both the thickness and length directions by power gradation laws under uniform distributed load was studied by the symmetric smoothed particle hydrodynamics method. In order to explore the behavior of this new type of structure in some further, a finite beam element is formulated in this paper for studying free and forced vibration of two-directional functionally graded sandwich (2D-FGSW) beams. The beams are considered to be formed from three layers, a homogeneous isotropic ceramic core and two FGM skin layers with material properties varying in both the thickness and length directions by power gradation laws. A refined shear deformation beam theory, in which the transverse displacement is split into bending and shear parts, is adopted to derive the element stiffness and mass matrices of the beam element. Thus, in addition to the vibration of the 2D-FGSW beams considered herein for the first time, the refined theory which allows to include the shear and rotary inertia effects by dividing the transverse displacement into bending and shear parts is also a new feature of this paper. The theory with the parabolic distribution of shear deformation in the beam thickness does not require a shear correction factor, and with the mentioned advantages, it has been widely adopted in vibration and buckling analysis of FGSW plates [14-17]. Using the derived formulation, natural frequencies and dynamic response of the beams with various boundary conditions to a harmonic load are computed, and the effects of material distribution, the layer thickness ratio and the aspect ratio on the vibration behavior of the beams are examined and highlighted.

## 2. 2D-FGSW Beam Model

A 2D-FGSW beam with a rectangular cross-section ( $b \times h$ ) as depicted in Fig. 1 is considered. The beam is assumed to form from three layers, namely a core of pure ceramic and two skin layers made of ceramic-metal FGM. In the figure, the  $x$ -axis is chosen on the mid-plane, and the  $z$ -axis is perpendicular to the mid-plane and directs upward. Denoting  $z_0$ ,  $z_1$ ,  $z_2$ , and  $z_3$  as the vertical coordinates of the bottom layer, layer interfaces, and the top layer, respectively.

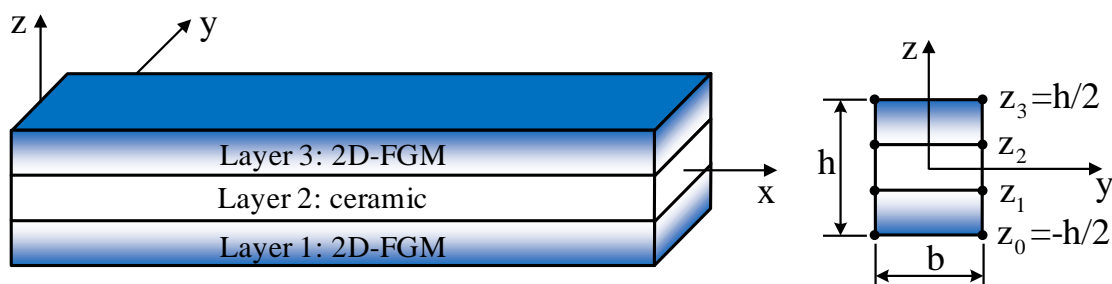


Fig. 1 Geometry of 2D-FGSW beam

The beam is considered to be made of ceramic and metal whose volume fraction varies in the thickness and length directions by power gradation laws as [13]

$$V_m = \begin{cases} \left( \frac{z-z_1}{z_0-z_1} \right)^{n_z} \left( 1 - \frac{x}{2L} \right)^{n_x} & \text{for } z \in [z_0, z_1] \\ 0 & \text{for } z \in [z_1, z_2] \\ \left( \frac{z-z_2}{z_3-z_2} \right)^{n_z} \left( 1 - \frac{x}{2L} \right)^{n_x} & \text{for } z \in [z_2, z_3] \end{cases} \quad (1)$$

and  $V_c = 1 - V_m$

where  $V_c$  and  $V_m$  are, respectively, the volume fraction of ceramic and metal;  $n_x$  and  $n_z$  are the grading indexes, defining variations of the constituent materials in the  $x$ - and  $z$ -directions, respectively. Noting that when  $n_x=0$  the beam deduces to the conventional 1D-FGSW beam with the material properties vary in the thickness direction only.

The effective property such as Young's modulus and mass density,  $P(x,z)$ , evaluated by the Voigt model is of the forms

$$P(x,z) = \begin{cases} (P_m - P_c) \left( \frac{z-z_1}{z_0-z_1} \right)^{p_z} \left( 1 - \frac{x}{2L} \right)^{p_x} + P_c & \text{if } z \in [z_0, z_1] \\ P_c & \text{if } z \in [z_1, z_2] \\ (P_m - P_c) \left( \frac{z-z_2}{z_3-z_2} \right)^{p_z} \left( 1 - \frac{x}{2L} \right)^{p_x} + P_c & \text{if } z \in [z_2, z_3] \end{cases} \quad (2)$$

where  $P_m$  and  $P_c$  are the properties of the metal and ceramic, respectively.

Based on the refined third-order shear deformation beam theory [6], the displacements in  $x$ - and  $z$ -directions,  $u_1(x,z,t)$  and  $u_3(x,z,t)$ , at any point of the beam are respectively given by

$$\begin{aligned} u_1(x,z,t) &= u(x,t) - z w_{b,x}(x,t) - \frac{4z^3}{3h^2} w_{s,x}(x,t) \\ u_3(x,z,t) &= w_b(x,t) + w_s(x,t) \end{aligned} \quad (3)$$

where  $u$ ,  $w_b$ ,  $w_s$  are the axial displacement, transverse bending and shear displacements of a point on the  $x$ -axis, respectively. In Eq. (3) and hereafter, a subscript comma is used to denote the derivative with respect to the followed variable, e.g.  $w_{s,x} = \partial w / \partial x$ . The strains resulted from Eq. (3) are of the forms

$$\begin{aligned} \varepsilon_x = u_{1,x} &= u_{,x} - z w_{b,xx} - \frac{4z^3}{3h^2} w_{s,xx}, \\ \gamma_{xz} = u_{1,z} + u_{3,x} &= \left( 1 - \frac{4z^2}{h^2} \right) w_{s,x} \end{aligned} \quad (4)$$

Assuming linearly elastic behavior, the constitutive equations for the beam are of the form

$$\sigma_x = \frac{E}{1-\nu^2} \varepsilon_x, \quad \tau_{xz} = \frac{E}{2(1+\nu)} \gamma_{xz} \quad (5)$$

where  $\nu$  is Poisson's ratio, assumed to be unchanged.

The strain energy ( $U$ ) resulted from Eqs. (4) and (5) is

$$\begin{aligned} U &= \frac{1}{2} \int_V (\sigma_x \varepsilon_x + \tau_{xz} \gamma_{xz}) dV = \frac{1}{2} \int_0^L [A_{11} u_{,x}^2 - 2A_{12} u_{,x} w_{b,xx} + A_{22} w_{b,xx}^2 - \frac{8}{3h^2} A_{23} u_{,x} w_{s,xx} \\ &\quad + \frac{8}{3h^2} A_{44} w_{b,xx} w_{s,xx} + \frac{16}{9h^4} A_{66} w_{s,xx}^2 + \left( B_{11} - \frac{8}{h^2} B_{22} + \frac{16}{h^4} B_{44} \right) w_{s,x}^2] dx \end{aligned} \quad (6)$$

where  $A_{11}, A_{12}, \dots, A_{66}, B_{11}, B_{22}, B_{44}$  are the beam rigidities, defined as

$$(A_{11}, A_{12}, A_{22}, A_{23}, A_{44}, A_{66}) = \int_A \frac{E}{1-\nu^2} (1, z, z^2, z^3, z^4, z^6) dA = \sum_{i=1}^3 \int_{z_{i-1}}^{z_i} \frac{bE}{1-\nu^2} (1, z, z^2, z^3, z^4, z^6) dz \quad (7)$$

and

$$(B_{11}, B_{22}, B_{44}) = \int_A \frac{E}{2(1+\nu)} (z, z^2, z^4) dA = \sum_{i=1}^3 \int_{z_{i-1}}^{z_i} \frac{bE}{2(1+\nu)} (1, z^2, z^4) dz \quad (8)$$

In Eqs. (6-8),  $V$  and  $A$  denote the volume and cross-sectional area of the beam, respectively. Because the effective Young modulus  $E$  varies in both the thickness and length directions, the rigidities in Eqs. (7) and (8) are functions of  $x$ .

The kinetic energy ( $T$ ) of the beam resulted from the displacement field in Eq. (3) is as follows

$$T = \int_0^L \left[ I_{11} (\dot{u}^2 + \dot{w}_b^2 + \dot{w}_s^2 + 2\dot{w}_b \dot{w}_s) - 2I_{12} \dot{u} \dot{w}_{b,x} + I_{22} \dot{w}_{b,x}^2 - \frac{8I_{34}}{3h^2} \dot{u} \dot{w}_{s,x} + \frac{8I_{44}}{3h^2} \dot{w}_{b,x} \dot{w}_{s,x} + \frac{16I_{66}}{9h^2} \dot{w}_{s,x}^2 \right] dx \quad (9)$$

in which  $I_{11}, I_{12}, I_{22}, I_{34}, I_{44}$ , and  $I_{66}$  are the mass moments, defined as

$$(I_{11}, I_{12}, I_{22}, I_{34}, I_{44}, I_{66}) = \int_A \rho(x, z) (1, z, z^2, z^3, z^4, z^6) dA = \sum_{i=1}^3 \int_{z_{i-1}}^{z_i} b\rho(x, z) (1, z, z^2, z^3, z^4, z^6) dz \quad (10)$$

The above mass moments, as the beam rigidities, also are functions of  $x$ . The potential ( $V$ ) of a harmonic load,  $F=F_0 \cos(\Omega t)$ , considered herein has a simple form

$$V = -F_0 \cos(\Omega t) (w_b + w_s) |_{x=x_F} \quad (11)$$

In the above equation, the subscript  $x=x_F$  means that the bending and shear transverse displacements are evaluated at the abscissa of the load  $F$ .

Equations of motion for the beam can be obtained by applying Hamilton's principle to Eqs. (6), (9) and (11). However, due to the rigidities and mass moment are functions of longitudinal coordinate  $x$ , the coefficients of such equation are dependent on  $x$ , and thus a closed-form solution is very difficult to obtain. A finite element formulation is developed below for computing the vibration characteristics of the beam.

### 3. Finite element formulation

A two-node beam element with length  $l$  is considered in this section. The element contains six degrees of freedom per node, and the vector of nodal displacements is given by

$$\mathbf{d} = \{ \mathbf{d}_u \quad \mathbf{d}_{wb} \quad \mathbf{d}_{ws} \}^T \quad (12)$$

where

$$\mathbf{d}_u = \{ u_1 \quad u_2 \}, \quad \mathbf{d}_{wb} = \{ w_{b1} \quad w_{b,x1} \quad w_{b2} \quad w_{b,x2} \}, \quad \mathbf{d}_{ws} = \{ w_{s1} \quad w_{s,x1} \quad w_{s2} \quad w_{s,x2} \} \quad (13)$$

are, respectively, the vectors of axial displacements, bending and shear transverse displacements at node 1 and node 2. In Eq. (12) and hereafter, a superscript "T" is used to denote the transpose of a vector or a matrix. It should be noted that the order of the nodal displacements is not necessary as in Eq. (12), but it is convenient to split the displacements into axial, bending and shear parts.

The displacements inside the element are interpolated from their nodal values according to

$$\begin{Bmatrix} u \\ w_b \\ w_s \end{Bmatrix} = \begin{bmatrix} \mathbf{N}_u & 0 & 0 \\ 0 & \mathbf{N}_{wb} & 0 \\ 0 & 0 & \mathbf{N}_{ws} \end{bmatrix} \begin{Bmatrix} \mathbf{d}_u \\ \mathbf{d}_{wb} \\ \mathbf{d}_{ws} \end{Bmatrix} \quad (14)$$

where  $\mathbf{N}_u$ ,  $\mathbf{N}_{wb}$  and  $\mathbf{N}_{ws}$  are the matrices of shape functions for  $u$ ,  $w_b$  and  $w_s$ , respectively. In the present work, the linear function is used for the axial displacement, while the Hermite cubic polynomials are employed for  $w_b$  and  $w_s$ . In this regard, we can write

$$\mathbf{N}_u = \{N_{u1} \ N_{u2}\} = \left\{ \frac{l-x}{l} \quad \frac{x}{l} \right\} \quad (15)$$

and

$$\mathbf{N}_w = \{N_{w1} \ N_{w2} \ N_{w3} \ N_{w4}\} \quad (16)$$

with

$$N_{w1} = 1 - 3\frac{x^2}{l^2} + 2\frac{x^3}{l^3}, \quad N_{w2} = x - 2\frac{x^2}{l} + \frac{x^3}{l^2}, \quad N_{w3} = 3\frac{x^2}{l^2} - 2\frac{x^3}{l^3}, \quad N_{w4} = -\frac{x^2}{l} + \frac{x^3}{l^2} \quad (17)$$

Using the above interpolation scheme, one can write the strain energy for the beam in the form

$$U = \frac{1}{2} \sum_{i=1}^{NE} \{\mathbf{d}\}_i^T \{\mathbf{k}\}_i \{\mathbf{d}\}_i \quad (18)$$

where  $NE$  is the total number of elements, and  $\mathbf{k}$  is the element stiffness matrix, which can be split into the sub-matrices as

$$\mathbf{k}_{(10 \times 10)} = \begin{bmatrix} \mathbf{k}_{aa} & \mathbf{k}_{ab} & \mathbf{k}_{as} \\ \mathbf{k}_{ab}^T & \mathbf{k}_{bb} & \mathbf{k}_{bs} \\ \mathbf{k}_{as}^T & \mathbf{k}_{bs}^T & \mathbf{k}_{ss} \end{bmatrix} \quad (19)$$

In the above,  $\mathbf{k}_{aa}$ ,  $\mathbf{k}_{bb}$ ,  $\mathbf{k}_{ss}$ ,  $\mathbf{k}_{ab}$ ,  $\mathbf{k}_{as}$ ,  $\mathbf{k}_{bs}$  are the stiffness matrices stemming from axial stretching, transverse bending, transverse shear and couplings of these terms. These sub-matrices can be obtained by twice differentiation of the strain energy  $U$  with respect the nodal displacements, for example

$$\mathbf{k}_{aa} = \frac{\partial^2 U}{\partial \mathbf{d}_u^2}, \quad \mathbf{k}_{ab} = \frac{\partial^2 U}{\partial \mathbf{d}_u \partial \mathbf{d}_{w_b}}, \quad \mathbf{k}_{bb} = \frac{\partial^2 U}{\partial \mathbf{d}_{w_b}^2} \quad (20)$$

Eq. (20) gives the sub-matrices in the following forms

$$\begin{aligned} \mathbf{k}_{aa} &= \int_0^l \mathbf{N}_{u,x}^T A_{11} \mathbf{N}_{u,x} dx, \quad \mathbf{k}_{ab} = -\int_0^l \mathbf{N}_{u,x}^T A_{12} \mathbf{N}_{w,x} dx, \quad \mathbf{k}_{as} = -\frac{4}{3h^2} \int_0^l \mathbf{N}_{u,x}^T A_{34} \mathbf{N}_{w,x,x} dx, \\ \mathbf{k}_{bb} &= \int_0^l \mathbf{N}_{w,x,x}^T A_{22} \mathbf{N}_{w,x,x} dx, \quad \mathbf{k}_{bs} = \frac{4}{3h^2} \int_0^l \mathbf{N}_{w,x,x}^T A_{44} \mathbf{N}_{w,x,x} dx, \\ \mathbf{k}_{ss} &= \frac{16}{9h^4} \int_0^l \mathbf{N}_{w,x,x}^T A_{66} \mathbf{N}_{w,x,x} dx + \int_0^l \mathbf{N}_{w,x}^T \left( B_{11} - \frac{8}{h^2} B_{22} + \frac{16}{h^4} B_{44} \right) \mathbf{N}_{w,x} dx \end{aligned} \quad (21)$$

Similarly, the kinetic energy of the beam can also be written in the form

$$T = \frac{1}{2} \sum_{i=1}^{NE} \{\dot{\mathbf{d}}\}_i^T \{\mathbf{m}\}_i \{\dot{\mathbf{d}}\}_i \tag{22}$$

where  $\dot{\mathbf{d}} = \partial \mathbf{d} / \partial t$  is the element nodal velocity, and  $\mathbf{m}$  is the element mass matrix which can be written in sub-matrices as

$$\mathbf{m}_{(10 \times 10)} = \begin{bmatrix} \mathbf{m}_{uu} & \mathbf{m}_{uw_b} & \mathbf{m}_{uw_s} \\ \mathbf{m}_{uw_b}^T & \mathbf{m}_{w_b w_b} & \mathbf{m}_{w_b w_s} \\ \mathbf{m}_{uw_s}^T & \mathbf{m}_{w_b w_s}^T & \mathbf{m}_{w_s w_s} \end{bmatrix} \tag{23}$$

The mass sub-matrices in the above equation are obtained by twice differentiation of the kinetic energy with respect to the associated nodal velocities and they have the following forms

$$\begin{aligned} \mathbf{m}_{uu}_{(2 \times 2)} &= \int_0^l \mathbf{N}_u^T I_{11} \mathbf{N}_u dx, \quad \mathbf{m}_{uw_b}_{(2 \times 4)} = -\int_0^l \mathbf{N}_u^T I_{12} \mathbf{N}_{w,x} dx, \quad \mathbf{m}_{uw_s}_{(2 \times 4)} = \int_0^l \left( \mathbf{N}_w^T I_{11} \mathbf{N}_w - \frac{4}{3h^2} \mathbf{N}_{u,x}^T I_{34} \mathbf{N}_{w,x} \right) dx, \\ \mathbf{m}_{w_b w_b}_{(4 \times 4)} &= \int_0^l \left( \mathbf{N}_w^T I_{11} \mathbf{N}_w + \mathbf{N}_{w,x}^T I_{22} \mathbf{N}_{w,x} \right) dx, \quad \mathbf{m}_{w_b w_s}_{(4 \times 4)} = \int_0^l \left( \mathbf{N}_w^T I_{11} \mathbf{N}_w + \frac{4}{3h^2} \mathbf{N}_{w,x}^T I_{44} \mathbf{N}_{w,x} \right) dx, \\ \mathbf{m}_{w_s w_s}_{(4 \times 4)} &= \int_0^l \left( \mathbf{N}_w^T I_{11} \mathbf{N}_w + \frac{16}{9h^4} \mathbf{N}_{w,x}^T I_{66} \mathbf{N}_{w,x} \right) dx \end{aligned} \tag{24}$$

Due to the rigidities and mass moments are functions of  $x$ , the integrals in Eqs. (21) and (24) are hardly computed explicitly. Gauss quadrature is employed herein to compute the stiffness and mass matrices.

With the introduced interpolations, the vector of nodal external load given by Eq. (11) can be written in the form

$$\mathbf{F}_{ex} = -F_0 \cos(\Omega t) \left\{ \begin{matrix} 0 & 0 & 0 & \dots & 0 & 0 & \mathbf{N}_w & \mathbf{N}_{w,x} & 0 & 0 & \dots & 0 & 0 & 0 & 0 \end{matrix} \right\}^T \tag{25}$$

element under loading

The matrix of the shape functions in the above equation is evaluated at  $x=x_F$ , the abscissa measured from the load to the left end of the element.

The equations of motion for the beam in term of finite element analysis can be written in the form [18]

$$\mathbf{M}\ddot{\mathbf{D}} + \mathbf{C}\dot{\mathbf{D}} + \mathbf{K}\mathbf{D} = \mathbf{F}_{ex} \tag{26}$$

where  $\mathbf{D}$ ,  $\dot{\mathbf{D}}$ ,  $\ddot{\mathbf{D}}$  are, respectively, the structural vectors of nodal displacements, velocities and accelerations;  $\mathbf{K}$ ,  $\mathbf{M}$ , and  $\mathbf{C}$  are structural stiffness, mass and damping matrices, respectively. Rayleigh damping, in which the damping matrix  $\mathbf{C}$  is proportional to a linear combination of mass and stiffness, is employed herein

$$\mathbf{C} = \alpha \mathbf{K} + \beta \mathbf{M} \tag{27}$$

where  $\alpha$  and  $\beta$  are, respectively, the mass and stiffness proportional Rayleigh damping coefficient, which are calculated from the critical damping ratio and the natural frequencies as

$$\alpha = 2\xi \frac{\omega_1 + \omega_2}{\omega_1 \omega_2}, \quad \beta = \frac{2\xi}{\omega_1 + \omega_2} \tag{28}$$

In the above,  $\xi$  is the damping ratio, taken by 5% for all numerical computation below.

## 4. Results and discussion

Using the derived finite element formulation, natural frequencies and dynamic response of the 2D-FGSW beam are computed, and numerical results are reported in this section. To this end, an FGSW beam formed from alumina (ceramic) and aluminum (metal) is considered. The material properties of the constituents are as follows [7]:

- (1)  $E_c=380$  MPa,  $\rho_c=3800$  kg/m<sup>3</sup>,  $\nu_c = 0.3$  for alumina
- (2)  $E_m=70$  MPa,  $\rho_m=2702$  kg/m<sup>3</sup>,  $\nu_m = 0.3$  for aluminum

For the convenience of discussion, the three numbers as proposed in [6] are used to indicate the layer thickness ratio, for example (2-1-2) means the thickness ratio of the bottom, core, and top layers is 2:1:2. Fig. 2 shows the variation of the effective Young's modulus and mass density in the thickness and length directions for (1-1-1) beam made of alumina and aluminum with  $n_x=n_z=0.5$  according to Eq. (2). It can be seen that Young's modulus and mass density continuously vary in both the thickness and length directions of the beam.

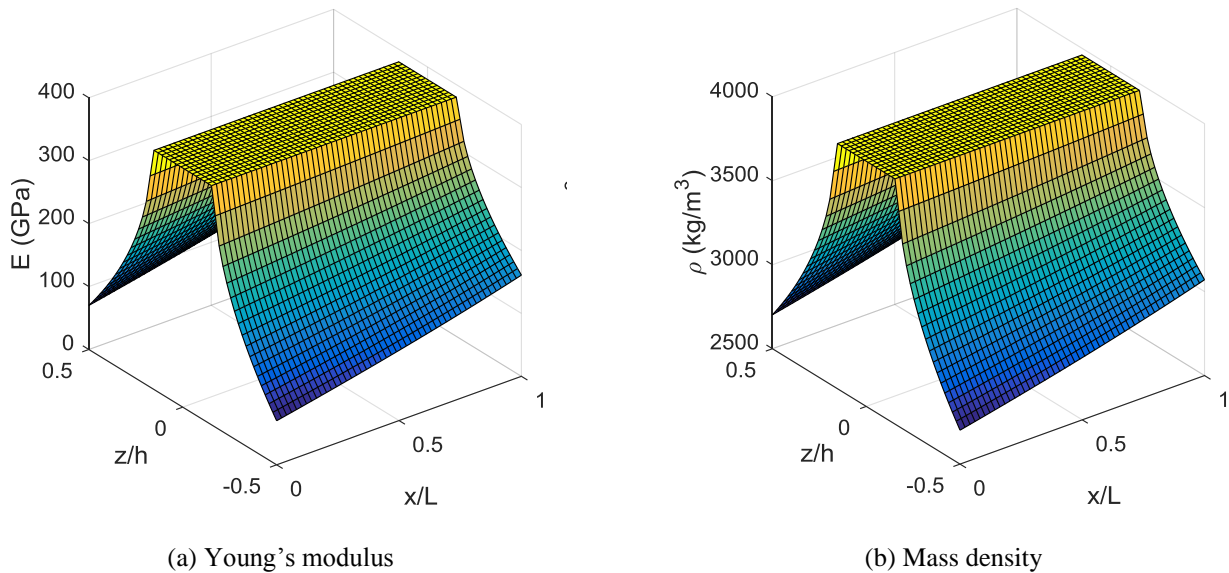


Fig. 2 Variation of Young's modulus and mass density for (1-1-1) beam with  $n_x=n_z=0.5$

### 4.1. Formulation verification

Before computing vibration characteristics of the beam, the derived formulation is necessary to confirm. Since there is no data on the vibration of the 2D-FGSW beam considered herein available in the literature, the comparison is carried out for the static bending of the beam as reported in [13]. Table 1 compares the maximum dimensionless deflection of the simply supported beam (SS beam) under uniform distributed load  $q_0$  obtained by the present finite element formulation with that of Karamanli [13] using the symmetric smoothed particle hydrodynamics method. Regardless of the grading indexes, the layer thickness ratio and the aspect ratio, the maximum deflection of the beam obtained in the present paper is in good agreement with that of Ref. [13]. The dimensionless deflection in Table 1 is defined as follows [13]

$$w^* = \frac{100E_m b h^3}{q_0 L^4} \max(w(x)) \quad (29)$$

where  $E_m$  is Young's modulus of metal.

Table 1 Comparison of maximum dimensionless deflection ( $w^*$ ) of SS beam under static uniform load

$n_x$	$n_z$	Source	$L/h = 5$			$L/h=20$			
			1-1-1	1-8-1	2-2-1	1-1-1	1-8-1	2-2-1	
0.1	0.1	Ref. [13]	10.7054	4.7401	10.9470	10.3994	4.4818	9.1047	
		Present	10.8634	4.8064	9.4128	10.4116	4.4848	9.1096	
	0.5	Ref. [13]	7.5039	4.2112	9.5412	7.2199	3.9561	6.5597	
		Present	7.6124	4.2698	6.8473	7.2273	3.9586	6.5680	
	1	Ref. [13]	6.0343	3.9030	6.9428	5.7613	3.6501	5.3608	
		Present	6.1185	3.9570	5.6327	5.7667	3.6525	5.3658	
	2	Ref. [13]	4.8871	3.6275	4.6673	4.6274	3.3772	4.4070	
		Present	4.9572	3.6775	4.7321	4.6313	3.3793	4.4101	
	0.5	0.1	Ref. [13]	8.4793	4.4862	5.7112	8.1706	4.4143	7.3680
			Present	8.6148	4.5492	7.6764	8.1964	4.2298	7.3839
		0.5	Ref. [13]	6.5069	4.0580	7.7882	6.2253	4.2331	5.7569
			Present	6.6011	4.1143	6.0408	6.2338	3.8040	5.7660
1		Ref. [13]	5.4735	3.8004	6.1257	5.2055	3.8068	4.9004	
		Present	5.5523	3.8534	5.1692	5.2114	3.5490	4.9064	
2		Ref. [13]	4.6040	3.5666	4.4251	4.3451	3.3169	4.1669	
		Present	4.6689	3.6155	4.4873	4.3491	3.3190	4.1706	
1		0.1	Ref. [13]	6.9827	4.2462	6.4602	6.6753	3.5515	6.1562
			Present	7.0975	4.3050	6.5600	6.7054	3.9922	6.1781
		0.5	Ref. [13]	5.7178	3.9088	5.3861	5.4388	3.9943	5.1050
			Present	5.8019	3.9608	5.4616	5.4499	3.6551	5.1153
	1	Ref. [13]	4.9904	3.6976	4.7624	4.7252	3.6570	4.4948	
		Present	5.0598	3.7487	4.8272	4.7288	3.4477	4.5000	
	2	Ref. [13]	4.3387	3.5031	4.1978	4.0816	3.2549	3.9396	
		Present	4.3982	3.5514	4.2549	4.0843	3.2566	3.9434	

4.2. Free vibration

The fundamental frequency parameters of the SS beam are listed in Tables 2 and 3 for various values of the grading indexes and the layer thickness ratio and two value of the aspect ratio,  $L/h=5$  and  $L/h=20$ , respectively. The frequency parameters in the tables (and below) are defined as follows

$$\mu_i = \frac{\omega_i L^2}{h} \sqrt{\frac{\rho_m}{E_m}} \tag{30}$$

where  $\omega_i$  is the  $i^{\text{th}}$  natural frequency of the beam.

Table 2 Fundamental frequency parameter ( $\mu l$ ) of SS beam with  $L/h = 5$

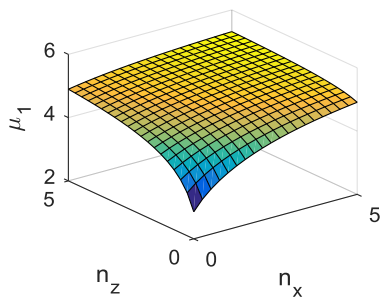
$n_x$	$n_z$	1-0-1	2-1-2	1-1-1	1-2-1	1-8-1	2-2-1
0	0.5	3.2500	3.3728	3.5186	3.7904	4.5227	3.7057
	1	3.5735	3.7297	3.8755	4.1105	4.6795	4.0189
	5	4.4615	4.5756	4.6582	4.7690	4.9899	4.7106
0.5	0.5	3.6300	3.7134	3.8194	4.0263	4.6176	3.9640
	1	3.8648	3.9816	4.0942	4.2804	4.7489	4.2086
	5	4.5673	4.6620	4.7311	4.8245	5.0125	4.7753
1	0.5	3.8922	3.9549	4.0378	4.2037	4.6942	4.1548
	1	4.0761	4.1687	4.2596	4.4123	4.8056	4.3538
	5	4.6520	4.7319	4.7906	4.8701	5.0315	4.8282
2	0.5	4.2427	4.2840	4.3402	4.4556	4.8093	4.4223
	1	4.3679	4.4318	4.4956	4.6043	4.8918	4.5629
	5	4.7785	4.8373	4.8807	4.9398	5.0609	4.9087
5	0.5	4.2427	4.2840	4.3402	4.4556	4.8093	4.4223
	1	4.3679	4.4318	4.4956	4.6043	4.8918	4.5629
	5	4.7785	4.8373	4.8807	4.9398	5.0609	4.9087

The effects of the grading indexes and the layer thickness ratio on the frequency of the beam are clearly seen from Tables 2 and 3. For a given value of the layer thickness ratio, the frequency parameter of the beam increases by the increase of the

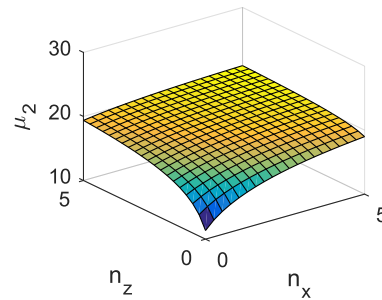
material grading indexes, regardless of the aspect ratio. This can be explained by the fact that the volume fraction of the metal, as seen from Eq. (1), is lower, and thus the ceramic percentage is larger for the beam associated with higher indexes  $n_x$  and  $n_z$ . Since Young's modulus of the ceramic is much higher than that of the metal, the rigidities of the beam with higher ceramic content are higher. The mass density of the beam with a higher ceramic content also larger, but for the constituent materials considered in this paper, the increase of the rigidities by increasing  $n_x$  and  $n_z$  is much faster than that of the mass moments. This explains the increase of the frequency when increasing the grading indexes. The layer thickness ratio, as seen from Table 2 and 3, also influences the increase of the frequency. For example, for the SS beam with  $L/h=20$  and a length index  $n_x=0.5$ , the frequency parameter  $\mu_1$  of the (1-0-1) beam increases 21.02% when increasing  $n_z$  from 0.5 to 5, but the corresponding value is 20.24%, 7.51%, and 8.44% for the (1-1-1), (1-2-1), and (1-8-1) beams, respectively. A careful examination of Table 2 and 3 shows that the increase of the frequency by increasing  $n_z$  depends upon the value of  $n_x$  also. For example, as seen from Table 2, the frequency parameter increases 20.35% when increasing  $n_z$  from 0.5 to 5 for (1-1-1) beam with  $n_x=0.5$ , but the corresponding value for the (1-1-1) beam with  $n_x=5$  is just 11.44%. In other words, the increase of the fundamental frequency by increasing the thickness index is smaller for the beam associated with a higher length index.

Table 3 Fundamental frequency parameter ( $\mu_1$ ) of SS beam with  $L/h = 20$

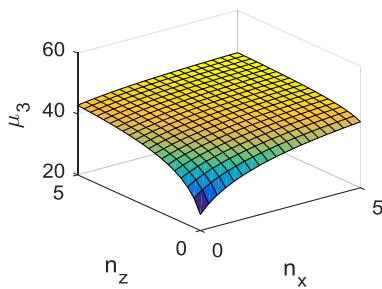
$n_x$	$n_z$	1-0-1	2-1-2	1-1-1	1-2-1	1-8-1	2-2-1
0	0.5	3.3781	3.4953	3.6472	3.9387	4.7473	3.8512
	1	3.7147	3.8768	4.0328	4.2889	4.9233	4.1906
	5	4.6783	4.8058	4.8987	5.0239	5.2748	4.9578
0.5	0.5	3.7880	3.8629	3.9727	4.1958	4.8533	4.1320
	1	4.0307	4.1510	4.2717	4.4760	5.0012	4.3988
	5	4.7962	4.9026	4.9806	5.0864	5.3005	5.0306
1	0.5	4.0732	4.1260	4.2112	4.3907	4.9391	4.3413
	1	4.2617	4.3563	4.4539	4.6222	5.0651	4.5594
	5	4.8911	4.9812	5.0476	5.1380	5.3220	5.0903
2	0.5	4.4581	4.4884	4.5450	4.6700	5.0686	4.6374
	1	4.5838	4.6477	4.7160	4.8365	5.1623	4.7923
	5	5.0334	5.1000	5.1494	5.2169	5.3554	5.1813
5	0.5	5.0070	5.0168	5.0398	5.0940	5.2756	5.0808
	1	5.0587	5.0853	5.1151	5.1690	5.3194	5.1496
	5	5.2595	5.2904	5.3134	5.3450	5.4104	5.3284



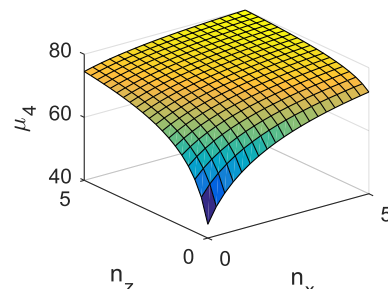
(a) The first parameter  $\mu_1$



(b) The second parameter  $\mu_2$



(c) The third parameter  $\mu_3$



(d) The fourth parameter  $\mu_4$

Fig. 3 Variation of the first four frequency parameters with grading indexes of (1-1-1) SS beam with  $L/h = 20$

The aspect ratio  $L/h$  also slightly influences the change of the frequency parameter and the change in the frequency parameter is not significant for the beam with a lower aspect ratio  $L/h$ . For example, the fundamental frequency parameter increases 17.17% for the (2-1-2) beam with  $n_x=1$  having  $L/h=20$  when increasing  $n_z$  from 0.5 to 5, but this increase reduces to 16.42% for the beam with  $L/h=5$ . Thus, the material gradation, the layer thickness ratio, and the aspect ratio are all important parameters which should be considered in designing the 2D-FGSW beam depends in order to achieve a beam with desired natural frequencies.

The effect of the grading indexes on the higher frequency parameters is illustrated in Fig. 3-5, where the variation of the first four natural frequency parameters with the grading indexes  $n_x$  and  $n_x$  is depicted for the SS, Clamped (CC) and Cantilever (CF) beams with a layer thickness ratio of (1-1-1) and an aspect ratio  $L/h=20$ , respectively. Similar to the fundamental frequency, the higher frequencies also increase by increasing the grading indexes  $n_x$  and  $n_z$ , regardless of the boundary conditions. The boundary conditions may affect the amplitude of the natural frequencies, but it hardly influences the dependence of the frequency parameters upon the material grading indexes.

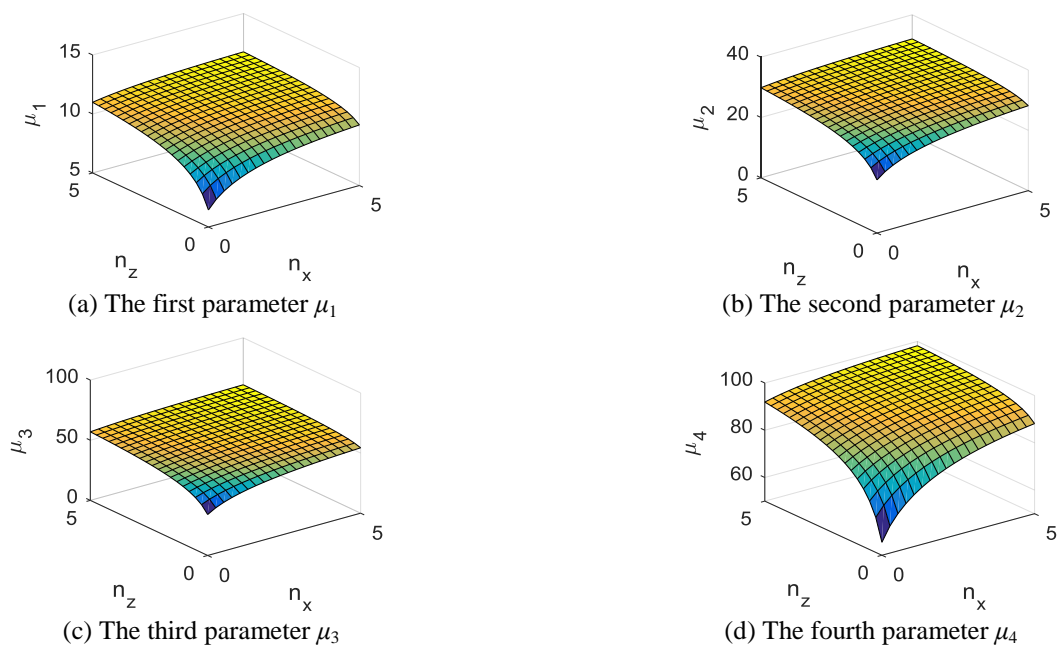


Fig. 4 Variation of the first four frequency parameters with grading indexes of (1-1-1) CC beam with  $L/h = 20$

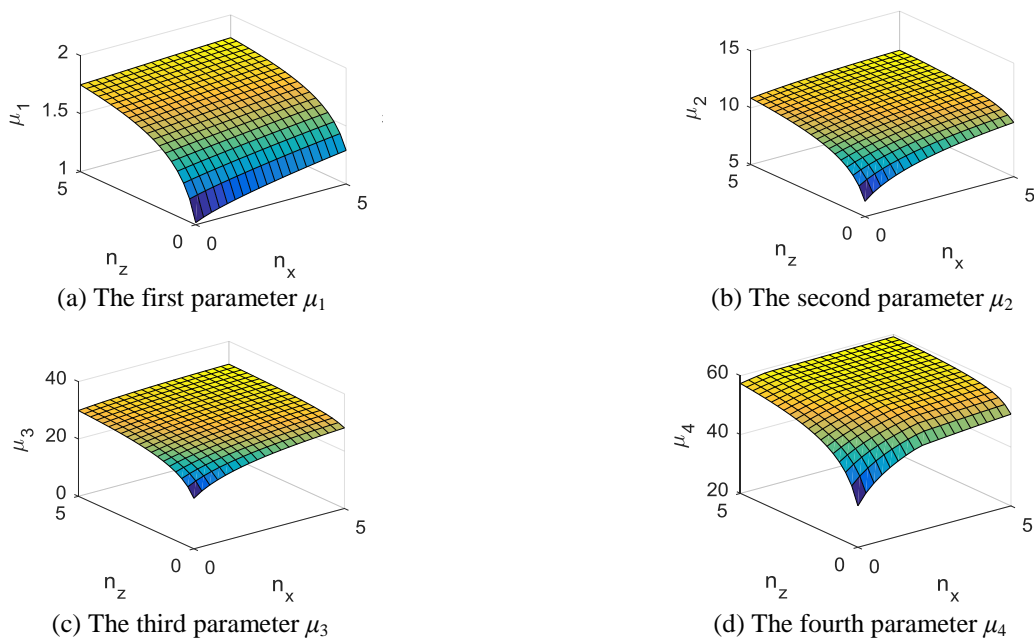


Fig. 5 Variation of the first four frequency parameters with grading indexes of (1-1-1) CF beam with  $L/h = 20$

4.3. Dynamic response

The dynamic response of the 2D-FGSW beam to a harmonic load  $P=P_0\cos(\Omega t)$  is investigated in this sub-section. In order to calculate the response of the beam, the average acceleration Newmark method is employed to solve Eq. (26). The beam with two types of boundary conditions, namely SS and CF beams, with a harmonic load acting at the mid-span and free end, respectively are considered herein. The variation of the dimensionless deflections with the time at the loaded points of the SS and CF beams with an aspect ratio  $L/h=20$  and a layer thickness ratio of (2-1-2) is illustrated in Fig. 6 and 7 for an excitation frequency  $\Omega=10$  rad/s, respectively. The deflections  $w^*$  in the figures are normalized by the static bending transverse displacements of the ceramic beam, that are

$$w^* = \frac{48E_c I}{PL^3} w_b(L/2) \quad \text{for SS beam} \tag{31}$$

$$w^* = \frac{3E_c I}{PL^3} w_b(L) \quad \text{for CF beam} \tag{32}$$

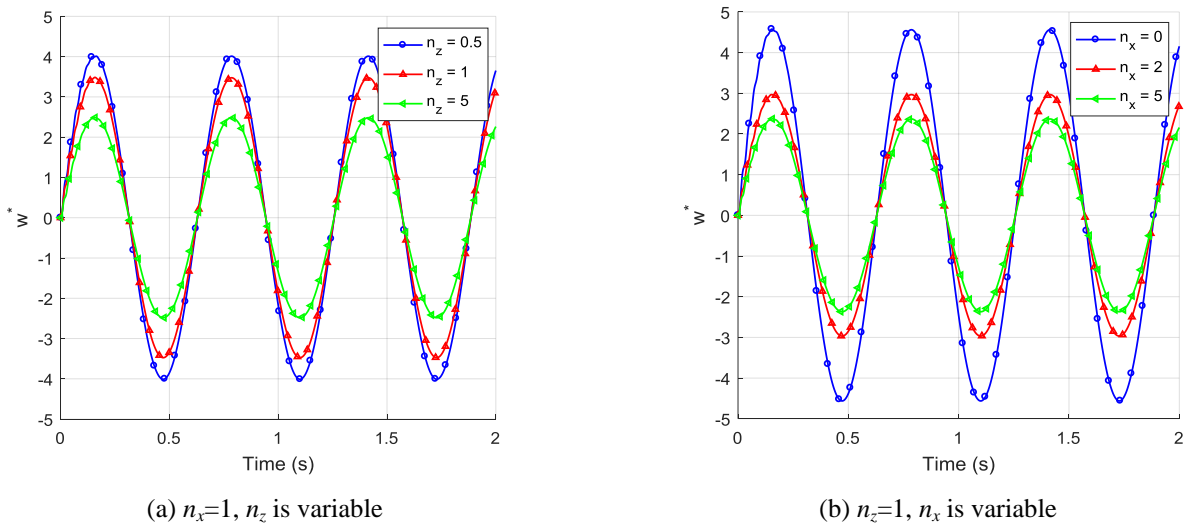


Fig. 6 Variation of mid-span dimensionless deflection with the time of SS (2-1-2) beam under harmonic load with  $\Omega=10$  rad/s acting at mid-span

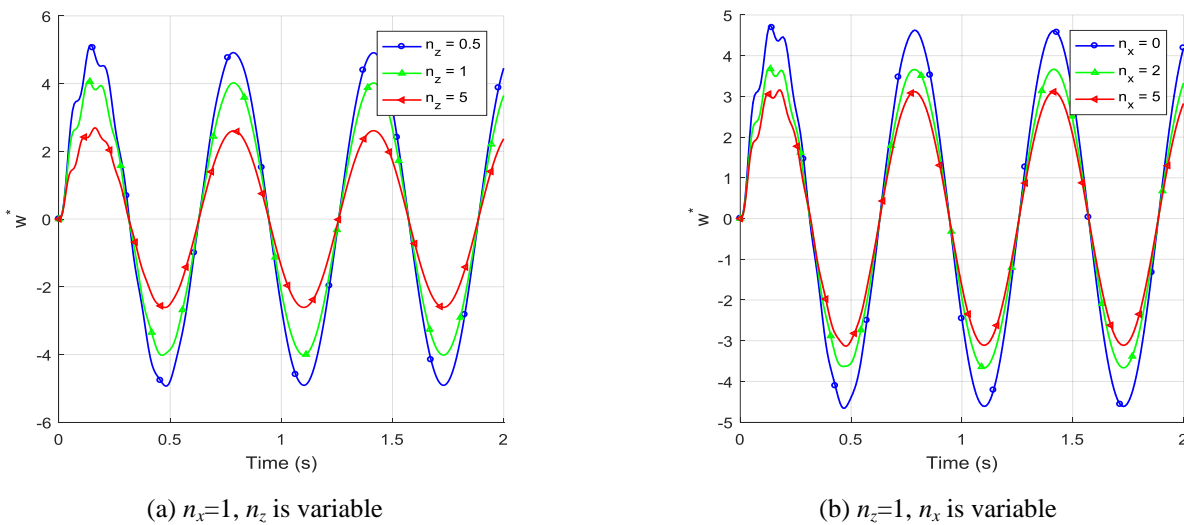


Fig. 7 Variation of dimensionless deflection at the free end with a time of CF (2-1-2) beam under harmonic load with  $\Omega=10$  rad/s acting at the free end

The effect of the grading indexes on the harmonic response of the beams can be seen from the figures, where the dynamic deflections are clearly decreased by increasing the material grading indexes  $n_x$  and  $n_z$ , regardless of the boundary conditions.

This effect can also be explained by the increase of ceramic content for the beam associated with the higher indexes, and this leads to higher rigidities for the beam associated with higher grading indexes, as explained above. As a result, the dynamic deflection of the beam is decreased by increasing the material grading indexes.

## 5. Conclusions

In this paper, a finite element formulation was developed for analyzing the free and forced vibration of 2D-FGSW beams. The beams were considered to be formed from three layers, a homogeneous ceramic core and two functionally graded skin layers with material properties varying in both the thickness and length directions by power gradation laws. Based on the refined third-order shear deformation theory, in which the transverse displacement is split into bending and shear parts, expressions for stiffness and mass matrices of a two-node beam element were derived and employed in computing natural frequencies and dynamic response of the beams. Numerical results obtained by using the formulation was compared with the published data to confirm the accuracy of the proposed formulation. A parametric study has been carried to highlight the effects of the material distribution, the layer thickness ratio and the aspect ratio on the vibration characteristics of the beams. The obtained results reveal that the material distribution and the layer thickness ratio of the beams play an important role on the vibration response of the 2D-FGSW beams. The numerical results of the present paper guide to design 2D-FGSW beams to achieve desired vibration characteristics. Though the paper examined only harmonic response of the beam, the finite element formulation developed herein can be employed to compute dynamic response of 2D-FGSW beams subjected to other types of dynamic loads as well.

## Conflicts of Interest

The authors declare no conflict of interest.

## Acknowledgement

This work was supported by Vietnam National Foundation for Science and Technology Development (NAFOSTED) under Grant no. 107.02-2018.23.

## References

- [1] M. Koizumin, "FGM activities in Japan," *Composites: Part B*, vol. 28, pp. 1-4, 1997.
- [2] S. C. Pradhan and T. Murmu, "Thermo-mechanical vibration of FGM sandwich beam under variable elastic foundations using differential quadrature method," *Journal of Sound and Vibration*, vol. 321, pp. 342-362, March 2009.
- [3] M. C. Amirani, S. M. R. Khalili, and N. Nemat. "Free vibration analysis of sandwich beam with FG core using the element free Galerkin method," *Composite Structures*, vol. 90, pp. 373-379, October 2009.
- [4] D. S. Mashat, E. Carrera, A. M. Zenkour, S. A. Al Khateeb, and M. Filippi, "Free vibration of FGM layered beams by various theories and finite elements," *Composites: Part B*, vol. 59, pp. 269-278, March 2014.
- [5] R. Bennai, H. A. Atmane, and A. Tounsi, "A new higher-order shear and normal deformation theory for functionally graded sandwich beams," *Steel and Composite Structures*, vol. 19, pp. 521-546, September 2015.
- [6] T. P. Vo, H.-T. Thai, T.-K. Nguyen, A. Maheri, and J. Lee, "Finite element model for vibration and buckling of functionally graded sandwich beams based on a refined shear deformation theory," *Engineering Structures*, vol. 64, pp. 12-22, April 2014.
- [7] T. P. Vo, H. -T. Thai, T. -K. Nguyen, F. Inam, and J. Lee, "A quasi-3D theory for vibration and buckling of functionally graded sandwich beams," *Composite Structures*, vol. 119, pp. 1-12, January 2015.
- [8] Z. Su, G. Jin, Y. Wang, and X. Ye, "A general Fourier formulation for vibration analysis of functionally graded sandwich beams with arbitrary boundary condition and resting on elastic foundations," *Acta Mechanica*, vol. 227, pp. 1493-1514, May 2016.
- [9] M. Şimşek, "Bi-directional Functionally Graded Materials (BDFGMs) for free and forced vibration of Timoshenko beams with various boundary conditions," *Composite Structures*, vol. 133, pp.968-978, December 2015.

- [10] Z. Wang, X. Wang, G. Xu, S. Cheng, and T. Zeng, "Free vibration of two-directional functionally graded beams," *Composite Structures*, vol. 135, pp.191-198, January 2016.
- [11] D. K. Nguyen, Q. H. Nguyen, T. T. Tran, and V. T. Bui, "Vibration of bi-dimensional functionally graded Timoshenko beams excited by a moving load," *Acta Mechanica*, vol. 228, pp.141-155, January 2017.
- [12] D. K. Nguyen and T. T. Tran, "Free vibration of tapered BFGM beams using an efficient shear deformable finite element model," *Steel and Composite Structures*, vol. 29, pp. 363-377, November 2018.
- [13] A. Karamanli, "Bending behaviour of two directional functionally graded sandwich beams by using a quasi-3d shear deformation theory," *Composite Structures*, vol. 174, pp. 70-86, August 2017.
- [14] M. A. A. Meziane, H. H. Abdelaziz, A. Tounsi, "An efficient and simple refined theory for buckling and free vibration of exponentially graded sandwich plates under various boundary conditions", *Journal of Sandwich Structures and Materials*, vol. 16, pp. 293-318, March 2014.
- [15] M. Bennoun, M. S. A. Houari, and A. Tounsi, "A novel five variable refined plate theory for vibration analysis of functionally graded sandwich plates", *Mechanics of Advanced Materials and Structures*, vol. 23, pp. 423-431, January 2016.
- [16] H. H. Abdelaziz, M. A. A. Meziane, A. A. Bousahla, A. Tounsi, S. R. Mahmoud, and A. S. Alwabli, "An efficient hyperbolic shear deformation theory for bending, buckling and free vibration of FGM sandwich plates with various boundary conditions," *Composite Structures*, vol. 25, pp. 693-704, December 2017.
- [17] F. Bourada, K. Amara, A. A. Bousahla, A. Tounsi, and S.R. Mahmoud, "A novel refined plate theory for stability analysis of hybrid and symmetric S-FGM plates", *Structural Engineering and Mechanics*, vol. 68, pp. 661-675, December 2018.
- [18] M. Géradin and R. Rixen, *Mechanical vibrations, Theory and application to structural dynamics*, 2nd edition. England; Chichester, John Wiley and Sons, 1997.



Copyright© by the authors. Licensee TAETI, Taiwan. This article is an open access article distributed under the terms and conditions of the Creative Commons Attribution (CC BY-NC) license (<https://creativecommons.org/licenses/by-nc/4.0/>).